Electronic Supplementary Material (ESI) for Journal of Materials Chemistry A.
This journal is © The Royal Society of Chemistry 2023

Supporting Information

Glucose oxidation assisted ammonia production via electrochemical dinitrogen reduction over $CoWO_4$

Akansha Chaturvedi, Divyani Gupta, Sukhjot Kaur, Kalpana Garg and Tharamani C. Nagaiah*

Chemical and reagents used: All analytical grade chemical and reagents were used with no further purification. Hydrated cobalt chloride ($CoCl_2.\ 6H_2O$;98%) and hydrated trisodium citrate ($Na_3C_6H_5O_7.2H_2O$; 99%(TSC)) were purchased from Alfa Aesar, hydrated sodium tungstate ($Na_2WO_4.2H_2O$; ≥99%) from Sigma- Aldrich and ethanol (≥99%) from Merck Millipore. Ammonium chloride (NH_4Cl, 99%), sodium sulphate (Na_2SO_4, 99%), Salicylic acid ($C_7H_6O_3$, 99.5%), potassium hydroxide (KOH, 85%), para-dimethylaminobenzaldeyde (p-$C_9H_{11}NO$, 99%), sodium nitroprusside (C_5FeN_6Na2O, 99%), sodium nitrate ($NaNO_3$, 99%), Sodium nitrite ($NaNO_2$, 98%), sulphanilamide ($C_6H_8N_2O_2S$, 99%), trisodium citrate ($Na_3C_6H_5O_7$), N-(1-Napthyl) ethylenediamine dihydrochloride ($C_{12}H_{14}N_2$, 99%), sodium hypochlorite solution (NaClO, 4-6%),), hydrazine monohydrate ($N_2H_4.H_2O$, 99%), hydrogen peroxide solution (H_2O_2, 5%) were obtained from LOBA chemie. High purity Ar gas (99.999%), $^{14}N_2$ (99.999%) and $^{15}N_2$ (99%) were obtained from Sigma. Deionised water used in the experiments was obtained from Millipore system (>12 MΩ cm^{-1})

Morphology and elemental analysis

The crystal structure of the prepared catalysts were examined by powdered X-ray diffraction spectroscopy. The spectra were recorded in a 2θ range of 10 to 70 ° using Cu-Kα radiation. The morphology of the catalyst was recorded using field emission- scanning electron microscopy (FESEM; ZEISS, ULTRA PLUS). EDS analysis was measured for elemental distribution (EDS; Oxford, INCAx-act, 51-ADD0013). UV-Vis measurements were recorded using Shimadzu UV-2600 spectrophotometer. The XPS measurements were evaluated by PHI VersaProbe II spectrometer, working at 15 kV and 35 mA under ultrahigh vacuum with Al Kα radiation (1486.6 eV). NMR spectra were recorded using a JEOL JNM-ECS 400 Hz spectrometer at ambient probe temperatures and referenced as follows: 1H: residual internal $CHCl_3$ 7.26 ppm; DMSO-d_6 2.50 ppm by applying water suppression.

Determination of ammonia

Indophenol blue method[1]

and 5% salicylic acid), 1 ml of oxidising solution (0.05 M NaClO) and 0.2 ml of catalyst solution (1% $Na_2(NO)(CN)_5.2H_2O$). UV-Vis spectrophotometric measurements were performed after 2 h of staining the sample with indophenol indicator. The calibration curve obtained showed good linear relationship between absorbance and concentration of NH_4Cl at a wavelength of 655 nm (Fig S7).

Measurement of NH_3 yield and Faradaic efficiency (F.E.)

NH_3 yield and F.E. were calculated by following equation:

$$NH_3\ yield = \frac{C \times V}{m \times t}$$

$$FE\ (\%) = \frac{3 \times C \times V \times 10^{-6} \times F}{17 \times Q}$$

Where *C* is concentration of NH_3 in µg/mL, *V* is volume of electrolyte in mL, *m* is mass loading of catalyst in mg, *t* is electrolysis time in h, *F* is faraday constant (96485 C/mol) and *Q* is total charge passed during electrolysis in C.

Nessler's reagent method[1]

The NH_3 yield evaluated by Indophenol blue technique, was validated by Nessler's test. Nessler's reagent was prepared by adding 2.5 g of mercuric iodide into 5 mL potassium iodide aqueous solution and then diluted to 20 mL by deionized water. After that 4 g of NaOH was added to the above prepared solution and named as Nessler's reagent. 5 mL of electrolyte was collected from cathodic chamber after e-NRR to which 0.25 mL of 500 g/L sodium potassium tartrate and 0.25 mL of Nessler's reagent was added. The UV-Vis. spectra of the above solution was measured after resting it for 10 min, with absorption estimation at λ=420 nm. The calibration curve was generated with known concentration of NH_4Cl arrangement, showing good linear relationship between absorbance and concentration.

Isotope labelling experiments[2]

To validate the true source of produced NH_3 during NRR, the isotope labelling experiment was performed by taking $^{15}N_2$ (Sigma-Aldrich 99 atom% ^{15}N) as the feeding gas. The $^{15}N_2$ gas was first passed through alkaline $KMnO_4$ followed by H_2SO_4 solution before purging to set-up cell and a definite amount of gas (200 mL) was supplied during the electrolysis at -0.35 V *vs*. RHE for 2 h. After electrolysis 10 ml of the electrolyte solution was taken and mixed with 1 M HCl and then concentrated. The ammonia produced was quantified by using ^1H nuclear magnetic resonance (^1H NMR) measurements with water suppression method. A single pulse sequence was applied during the relaxation delay of 1 s with a total number of 8000 transient scans and an acquisition time of 2.18 s. From the concentrated electrolyte sample, 0.7 mL of the resultant solution was taken and 0.2 mL of DMSO- d_6 was added as an internal standard to attain appropriate lock signal and 0.125 mL of maleic acid was added for quantification purpose. Similarly other samples ($^{14}N_2$ and Ar saturated) were tested. Calibration curves were extracted for various concentrations of standard $^{14}NH_4Cl$ and $^{15}NH_4Cl$ solutions ranging between 1 to 3 ppm with reference to maleic acid as a standard with a total number of 1024 scans.
Further, the quantification was executed by means of liquid chromatography-mass spectroscopy (LC-MS) technique by following the reported procedure.[3] Briefly 150 µL of phenol solution was mixed with 30 µL each of sodium hypochlorite and sodium nitroprusside . The above solution mixture was then added into 1.5 mL of the NH_4^+ containing standard and sample solution to generate Indophenol blue. After which 15 µL of 10 M HCl was added in order to convert the complex into Indophenol red, which was then extracted by addition of ethyl acetate (1.5 mL) from organic layer. The organic layer was separated from aqueous layer and ethyl acetate was completely evaporated, thereafter the indophenol red was re-dissolved in methanol for LC-MS.

Determination of hydrazine (N_2H_4)

Watt and Chrisp method[4] was used for the detection of N_2H_4. The calibration curves were obtained for different concentration from 0.0 ppm to 1.0 ppm of $N_2H_4.H_2O$ solution. 3 ml of sample or standard solution was mixed with 3 ml of colouring agent (5.99 g p-$C_9H_{11}NO$, 30 ml HCl and 300 ml C_2H_5OH). The UV -vis spectra of the above solution was measured after resting it for 10 min, in the range of 600 to 400 nm. The obtained plot shows good linear relation between absorbance *vs*. concentration of N_2H_4 (Fig. S8).

Determination of Nitrite (NO_2^-)[5]

Nitrite concentration was determined quantitatively at a wavelength of 540 nm using UV-Vis spectrophotometer. Standard solution of $NaNO_2$ of different concentration from 2 µg L^{-1} to 100 µg L^{-1} were made. The colouring reagent 1 was prepared by dissolving 0.5 g of sulfanilamide in 50 mL of 2 M HCl solution. Reagent 2 was prepared by dissolving 20 mg of N-(1-Naphthyl) ethylenediamine dihydrochloride in 20 mL water. To the 5 mL standard or sample solution, 100 µL of reagent 1 was added and after resting for about 10 min, 100 µL of reagent 2 was added to the above solution. The solution was kept at rest for 30 min and then its UV-Vis measurements were conducted in the range of 450 to 650 nm. The concentration-absorbance standard curves were then plotted, showing a good linear relationship. (Fig. S11)

Determination of Nitrate (NO_3^-)[5]

The content of nitrate was measured using UV-Vis spectrophotometer at wavelength of 220 nm. Calibrations curves were plotted for standard solution of $LiNO_3$ with different concentration from 0.2 ppm to 5 ppm in the range of 200 -280 nm. 100 µL of 0.1 M HCl was added to 5 mL of standard or sample solution and after resting it for 5 min, UV- vis measurements were taken showing decent linear relation of absorbance versus NO_3^- concentration. (Fig. S12).

Determination of NO_x in feeding gas-supplies[6, 7]

The NO_x (NO/NO_2) was captured in alkaline $KMnO_4$ solution, as it gets oxidised to NO_3^-/NO_2^- and was quantified using UV-Vis spectrophotometry before and after passing through the purification apparatus. Whereas the trace N_2O was quantified using GC-MS in SIM (selected ion monitoring) mode with m/z value of 44. The data acquisition settings were adjusted at a column oven temperature of 40 °C and an injection temperature of 150 °C. The column flow was kept constant at 0.99 mL min^{-1}, with an ion source temperature of 200 °C and an interface temperature of 220 °C.

Electrochemical surface area (ECSA)

Electrochemical active surface area was measured by performing CV in non-faradaic region from -0.2 V to -0.05 V *vs*. RHE at various scan rate of 20 to 280 mV s^{-1}. Capacitance double layer (C_{dl}) was determined by the slope of average current density ((Ia+Ic)/2) *vs*. scan rate. The ECSA was determined by dividing C_{dl} with specific capacitance of the flat standard surface (20-60 µF cm^{-2}). For our present study we considered it to be 40 µF cm^{-2}. Roughness factor was then measured by dividing ECSA with geometrical surface area.

ECSA = C_{dl} /C_s

where C_s is specific capacitance

Roughness factor (a.u.) = ECSA/ geometrical surface area

where geometrical surface area is 0.0314 cm^{-2}.

Determination of hydrogen production:

H_2 evolved during NRR at particular potentials were detected by a gas chromatograph (GC, SHIMADZU, GC 2030). High purity N_2 (99.999%) was continuously purged in the cathodic compartment of H-cell during NRR. A SHIMADZU Rt-Q-BOND column was installed in GC having two detectors, namely, a thermal conductivity detector (TCD) and a flame ionization detector (FID) to measure H_2. The carrier gas used was N_2. Formulas mentioned below are used for quantification of hydrogen produced.

$$H_2\ yield = \frac{yield\ (mmol)}{t\ (h) \times m_{cat.}(mg)}$$

$$Selectivity\ (\%) = \frac{Experimental\ H_2\ \times 100}{Theoretical\ \ H_2}$$

Turn over frequency (TOF) for $CoWO_4$ (12 h) calculation:

$$Turn\ over\ number\ (TON) = \frac{NH_3\ yield\ (mg)}{Catalyst\ loading\ (mg)}$$

$$TOF = \frac{TON}{Time\ (h)}$$

Where, NH_3 yield is obtained from quantification of NH_3 after electrolysis, Time is the total duration of electrolysis in hours.

Hence TON and TOF for $CoWO_4$ is calculated as follows:

$$TON = \frac{0.048}{0.036} = 1.34$$

$$TOF = \frac{1.34}{2} = 0.67$$

$$TOF = 0.67\ h^{-1}$$

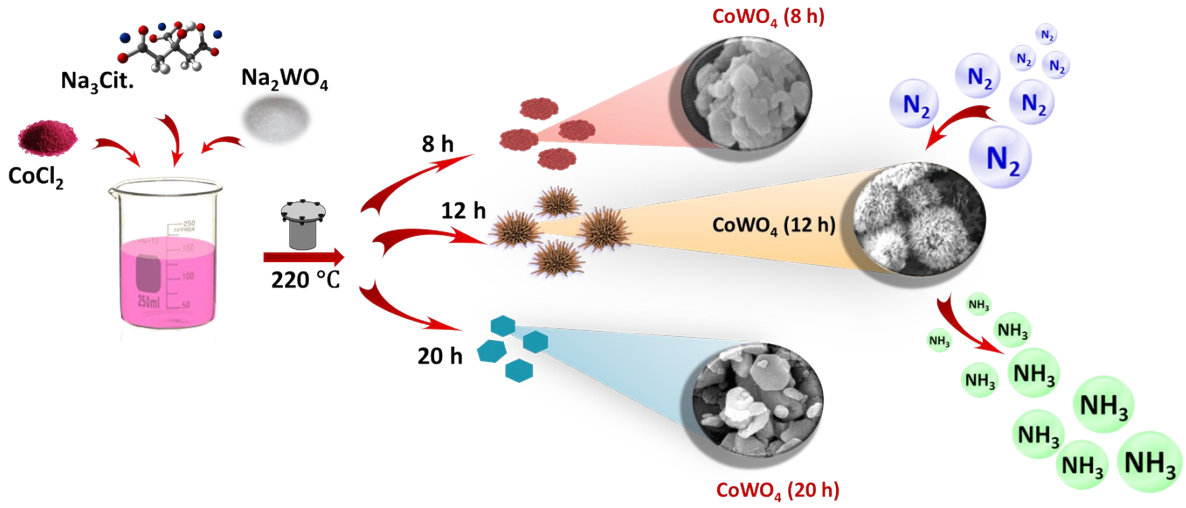

Scheme S1 Schematic representation of synthesis of $CoWO_4$ at different time (8, 12 and 20 h).

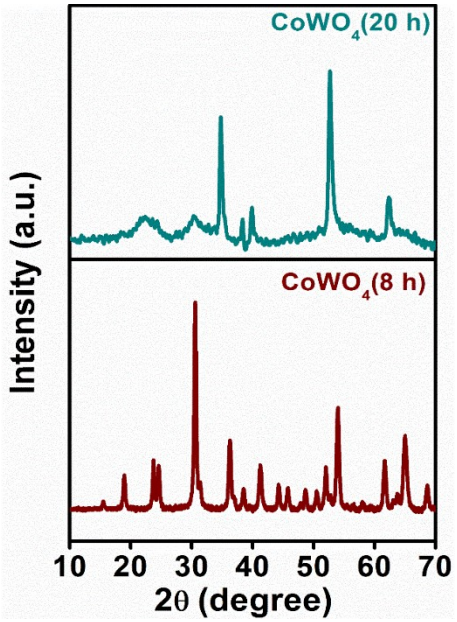

Fig. S1 XRD pattern for $CoWO_4$ (8 h), and $CoWO_4$ (20 h) catalysts.

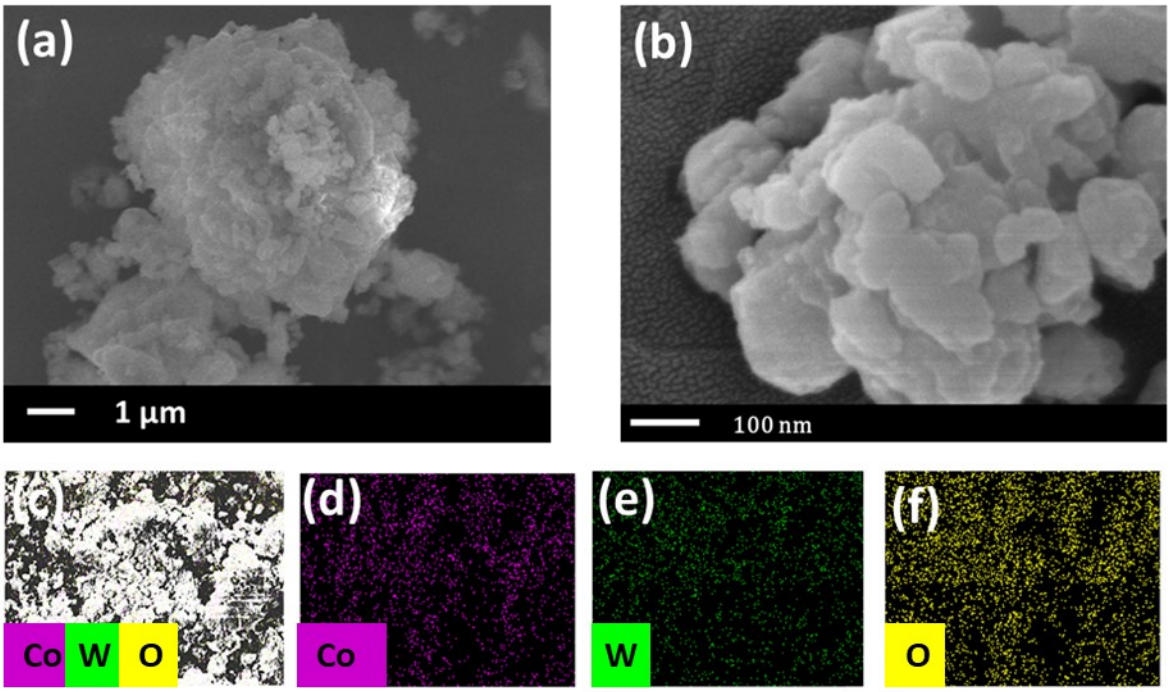

Fig. S2 (a),(b) FE-SEM images for $CoWO_4$ (8 h) catalyst with different magnification and EDS dot mapping images for $CoWO_4$ (8 h) catalyst showing presence of (c) all the elements in scanned area, (d) Co, (e) W and (f) O elements respectively.

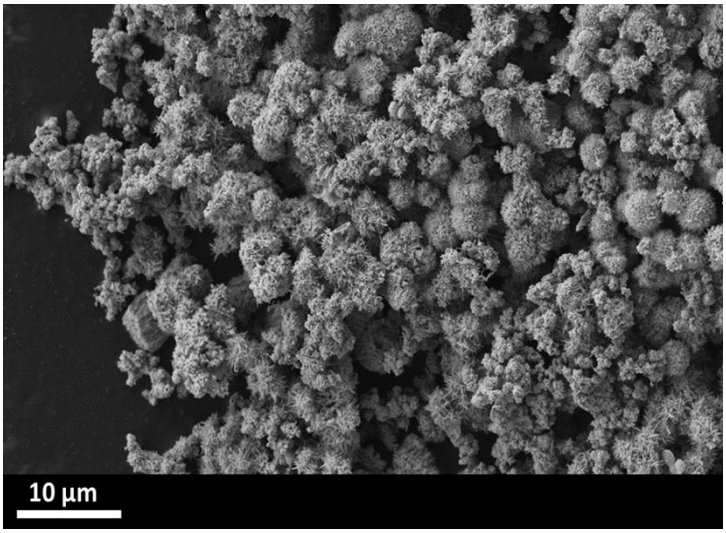

Fig. S3 FE-SEM images for $CoWO_4$ (12 h) catalyst with 10 µm magnification

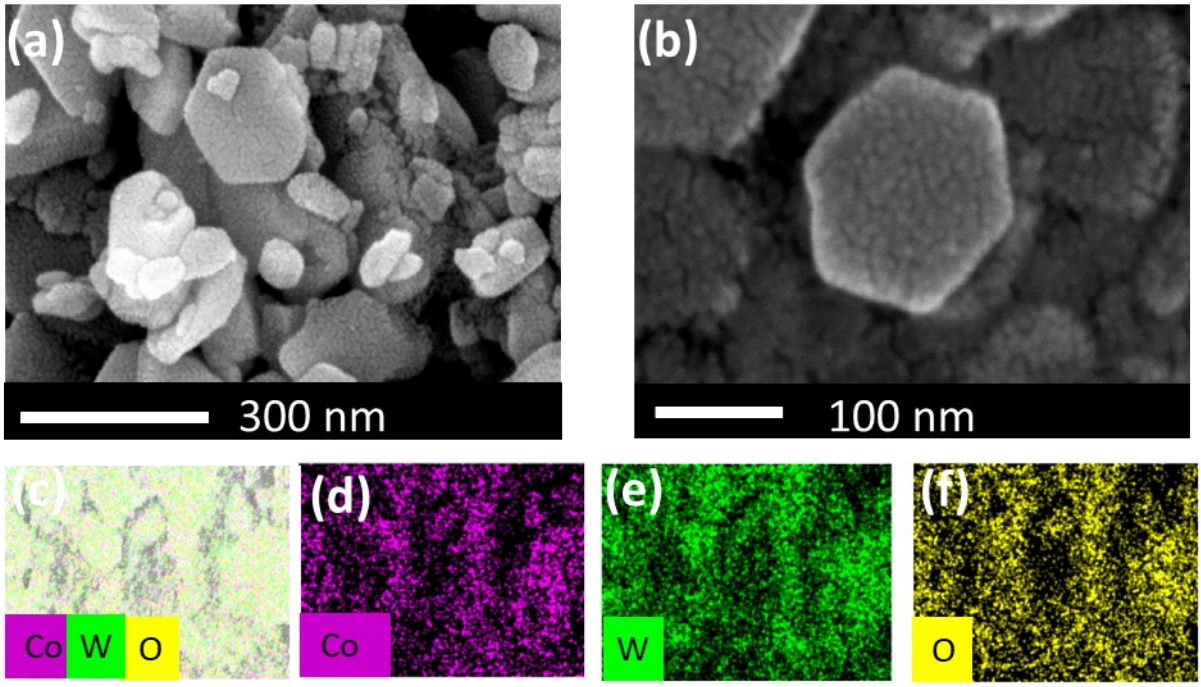

Fig. S4 (a),(b) FE-SEM images for $CoWO_4$ (20 h) catalyst with different magnification and EDS dot mapping images for $CoWO_4$ (20 h) catalyst showing presence of (c) all the elements in scanned area, (d) Co, (e) W and (f) O elements respectively.

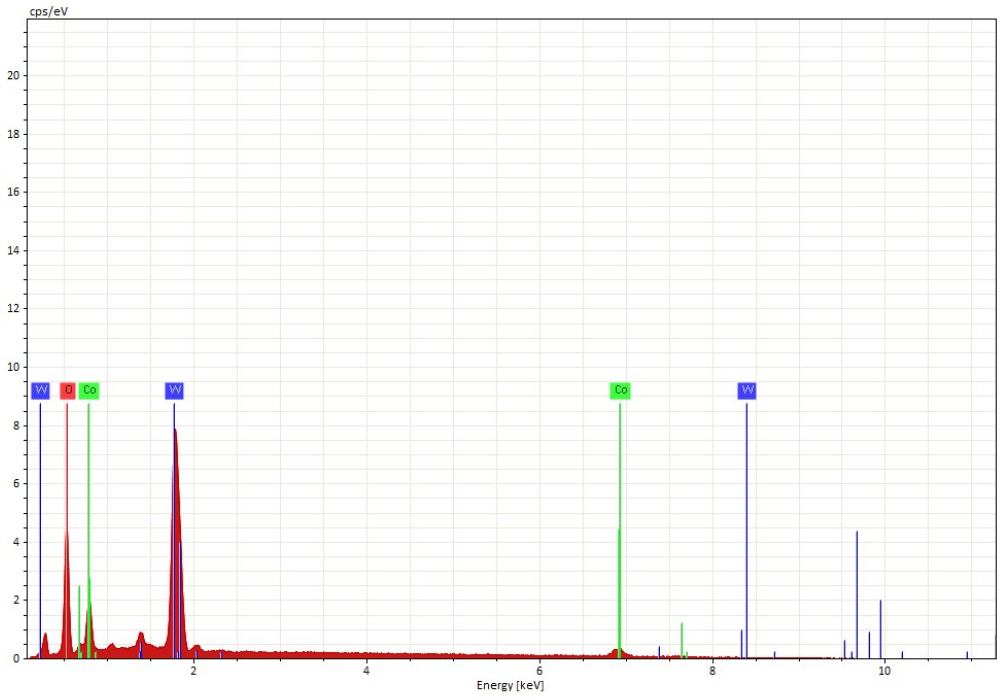

Fig. S5 EDS spectra of $CoWO_4$ (12 h) showing presence of Co, W and O.

Table S1: EDS composition analysis (%) for $CoWO_4$ (8 h), $CoWO_4$ (12 h), and $CoWO_4$ (20 h)						
$CoWO_4$ (8 h)			**$CoWO_4$ (12 h)**		**$CoWO_4$ (20 h)**	
Elements	Weight %	Atomic %	Weight %	Atomic %	Weight %	Atomic %
Cobalt	16.16	16.99	10.648	8.822	29.87	21.02
Tungsten	19.73	64.71	65.145	17.301	43	69.18
Oxygen	64.11	18.30	24.208	73.877	26.69	9.80

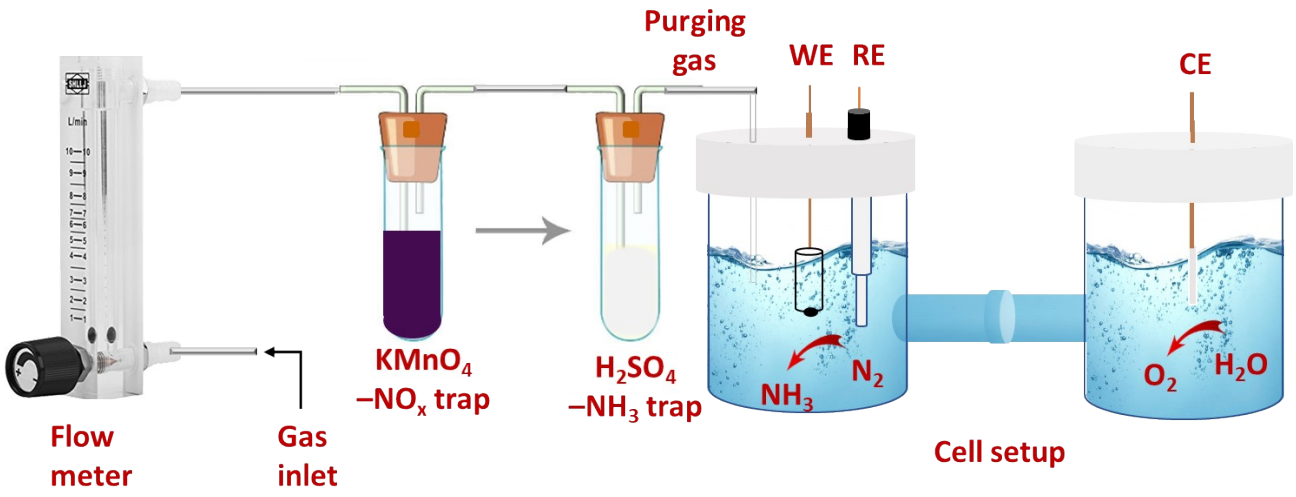

Fig. S6 Schematic representation of electrochemical cell set-up for NRR containing gas purification through alkaline $KMnO_4$ followed by dilute H_2SO_4 trap solution.

Table S2: Determination of NO_x in feeding gas-supplies before and after purification.				
	Feeding gas	**Ar**	**$^{14}N_2$**	**$^{15}N_2$**
Before purification	**NO/NO_2 (UV-Vis spectrophotometry)**	0.6 ppm	1.1 ppm	1.2 ppm
	N_2O (chromatography)	<0.01	0.06 ppm	0.07 ppm

		ppm		
After purification	**NO/NO_2 (UV-Vis spectrophotometry)**	-	<0.01 ppm	<0.01 ppm
	N_2O (chromatography)	NA	<0.01 ppm	<0.01 ppm

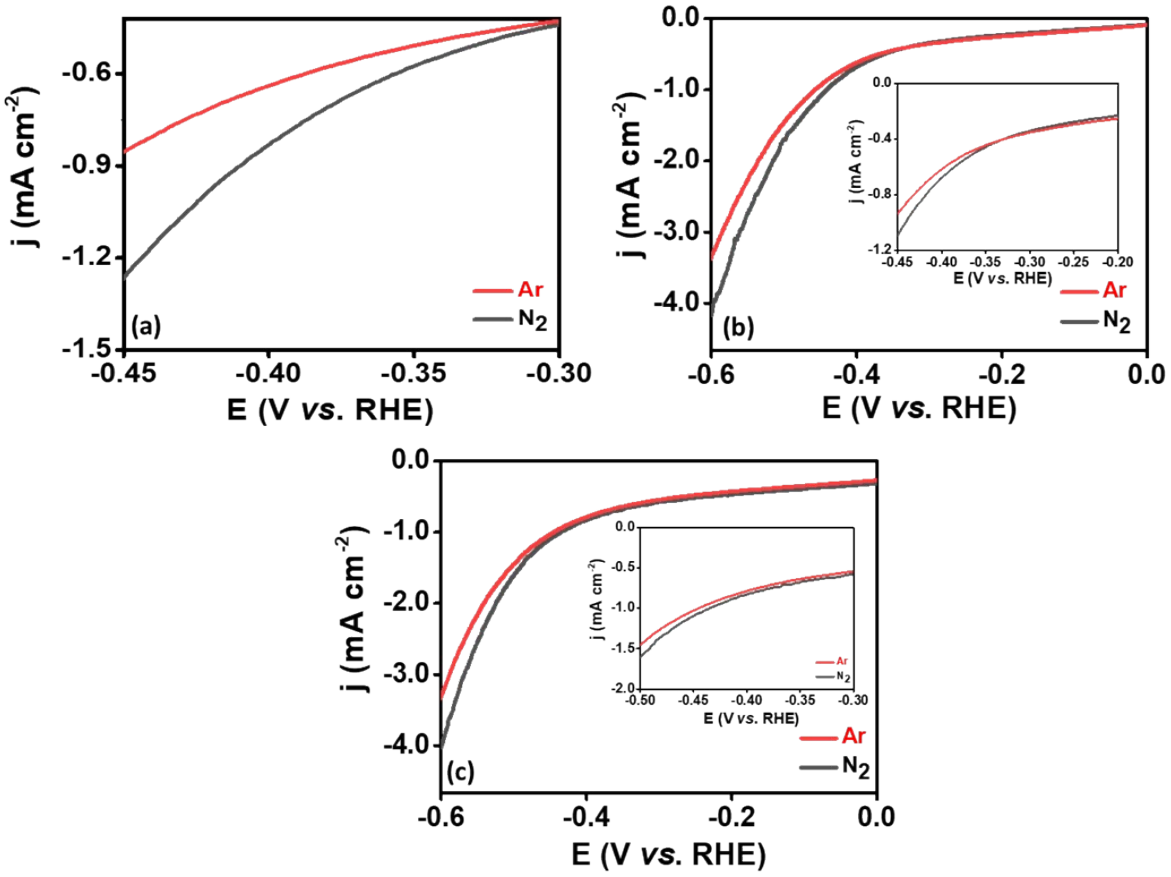

Fig. S7 Linear sweep voltammetry (LSV) for (a) $CoWO_4$ (12 h) (zoomed part extracted from Fig 3(a)), (b) $CoWO_4$ (8 h) and (c) $CoWO_4$ (20 h) catalyst in N_2 saturated and Ar-saturated 0.1 M KOH solution.

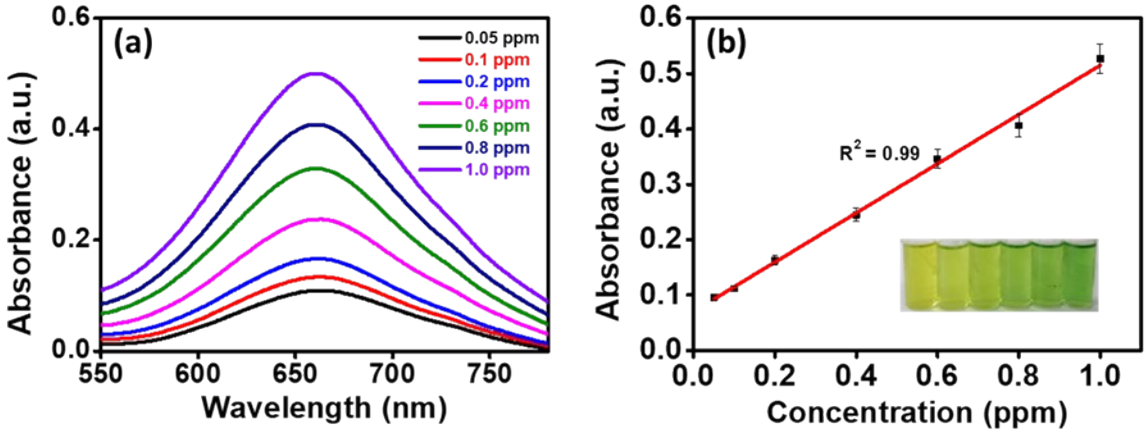

Fig. S8 UV-Vis spectra of indophenol blue method for different concentration of NH_3 and its corresponding calibration curve for measurement.

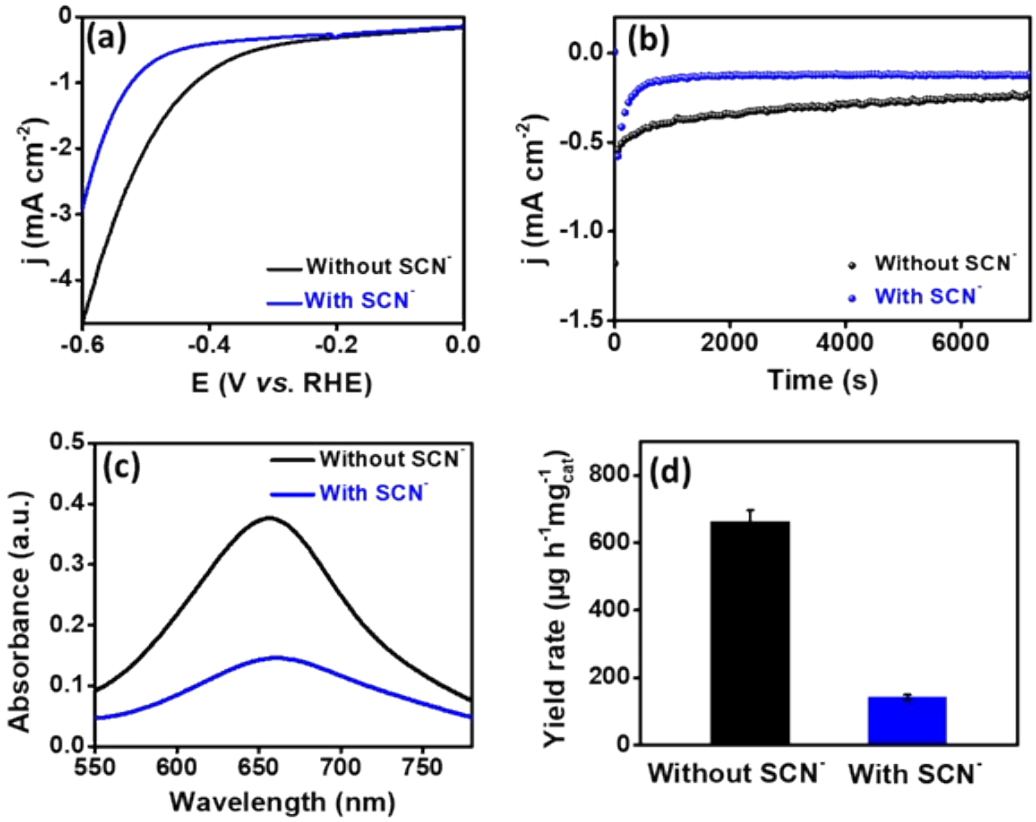

Fig. S9 (a) Linear sweep voltammograms for catalysts in N_2 saturated 0.1 M KOH electrolyte solution with and without KSCN, (b) chronoamperometric curves obtained at -0.35 V *vs*. RHE for 2 h in the presence and absence of KSCN, (c) UV-Vis spectrum obtained by the indophenol blue method and (d) bar graph representation of the NH_3 yield rate calculated for $CoWO_4$ (12 h). (WE: GCE; RE: Hg/HgO/1 M NaOH; CE: graphite rod).

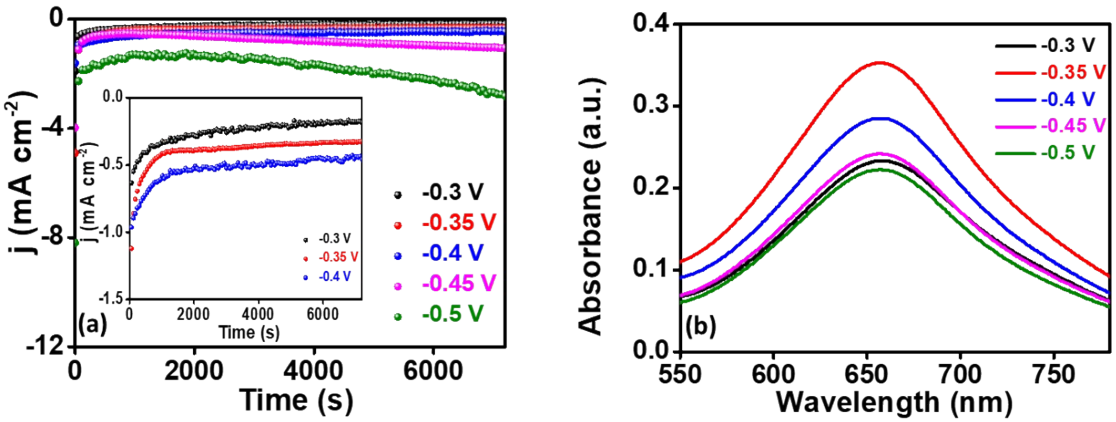

Fig. S10 (a) Chronoamperometry curves for different potential from -0.3 V to -0.5 V *vs*. RHE. and (b) its corresponding UV-Vis absorption spectra for $CoWO_4$ (8 h) catalyst.

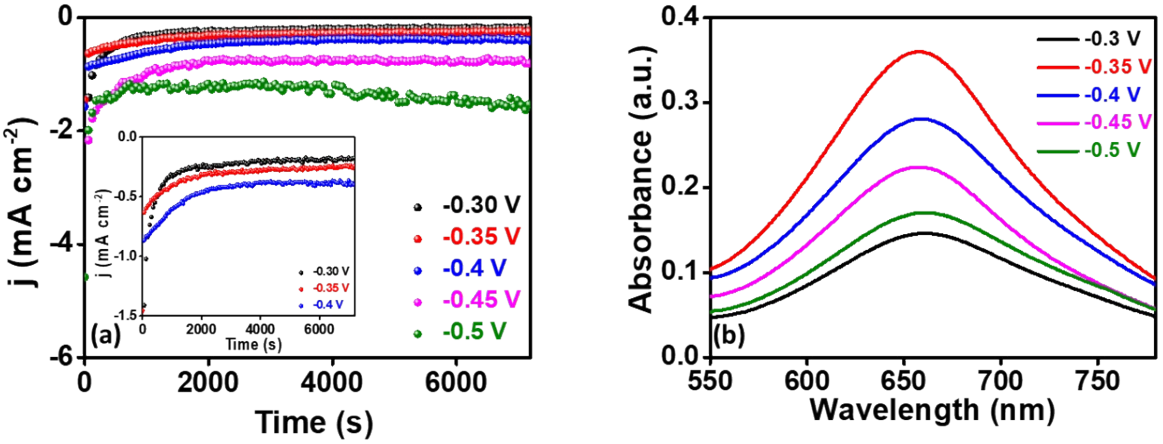

Fig. S11 (a) Chronoamperometry curves for different potential from -0.3 V to -0.5 V *vs.* RHE. and (b) its corresponding UV-Vis absorption spectra for $CoWO_4$ (20 h) catalyst.

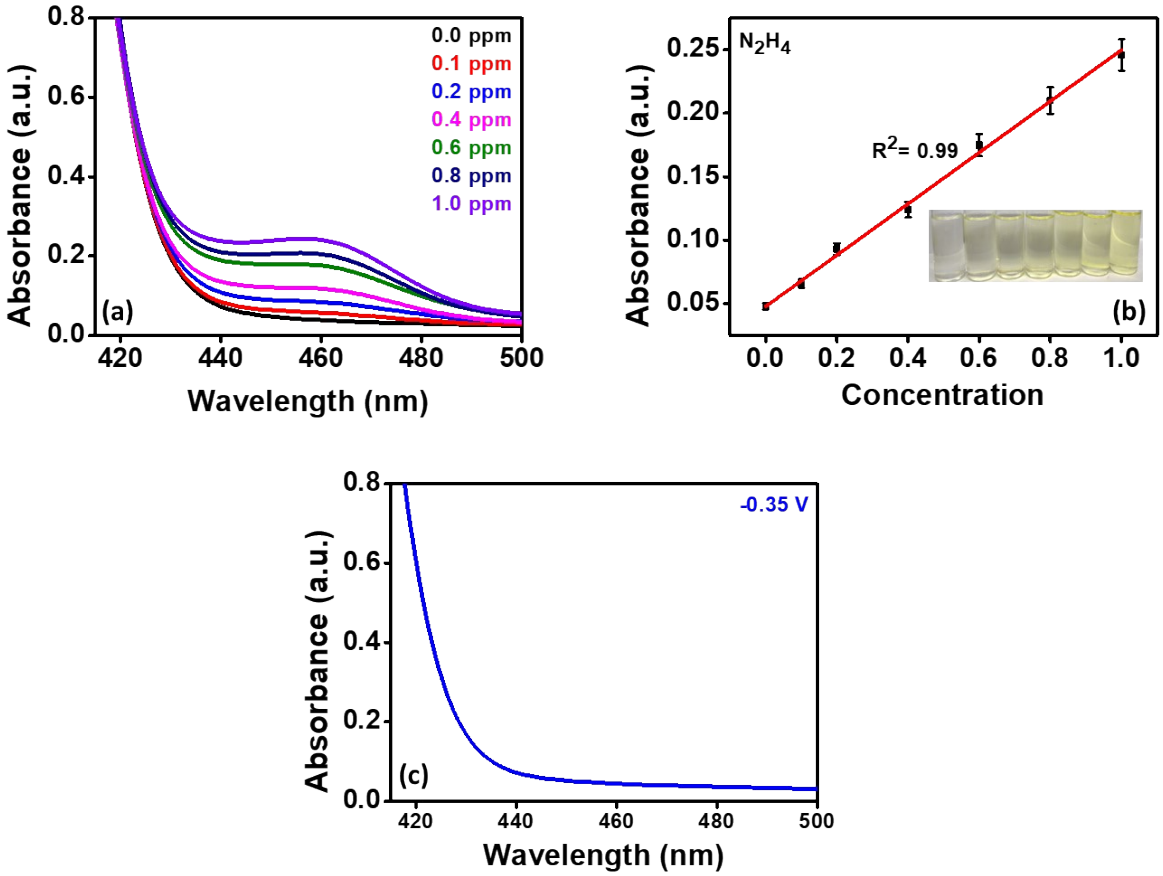

Fig. S12 (a) UV-Vis absorption spectra for various concentration of N_2H_4 (b) Corresponding calibration curve for determining N_2H_4 concentration (c) UV-Vis absorption spectra of electrolyte measured by Watt and Chrisp after NRR electrolysis at -0.35 V *vs.* RHE.

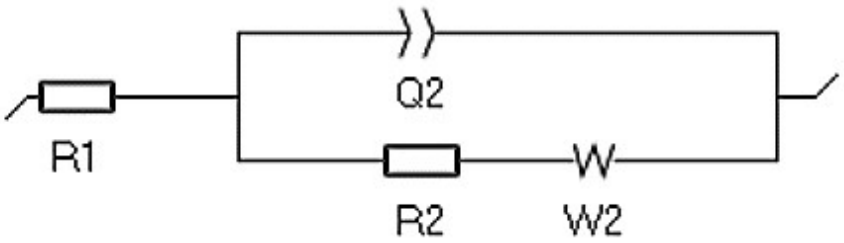

Fig. S13 Equivalent circuit (R1+Q2/(R2+W2)) for Nyquist plots of catalysts extracted from 4c.

Table S3: Electrochemical impedance analysis				
S.No.	**Catalyst**	**R_S (Ω)**	**R_p (Ω)**	**R_{ct} (Ω)**
1	$CoWO_4$ (8 h)	19.4	109.3	89.9
2	$CoWO_4$ (12 h)	17.47	93.29	75.82
3	$CoWO_4$ (20 h)	24.5	143.09	119.4

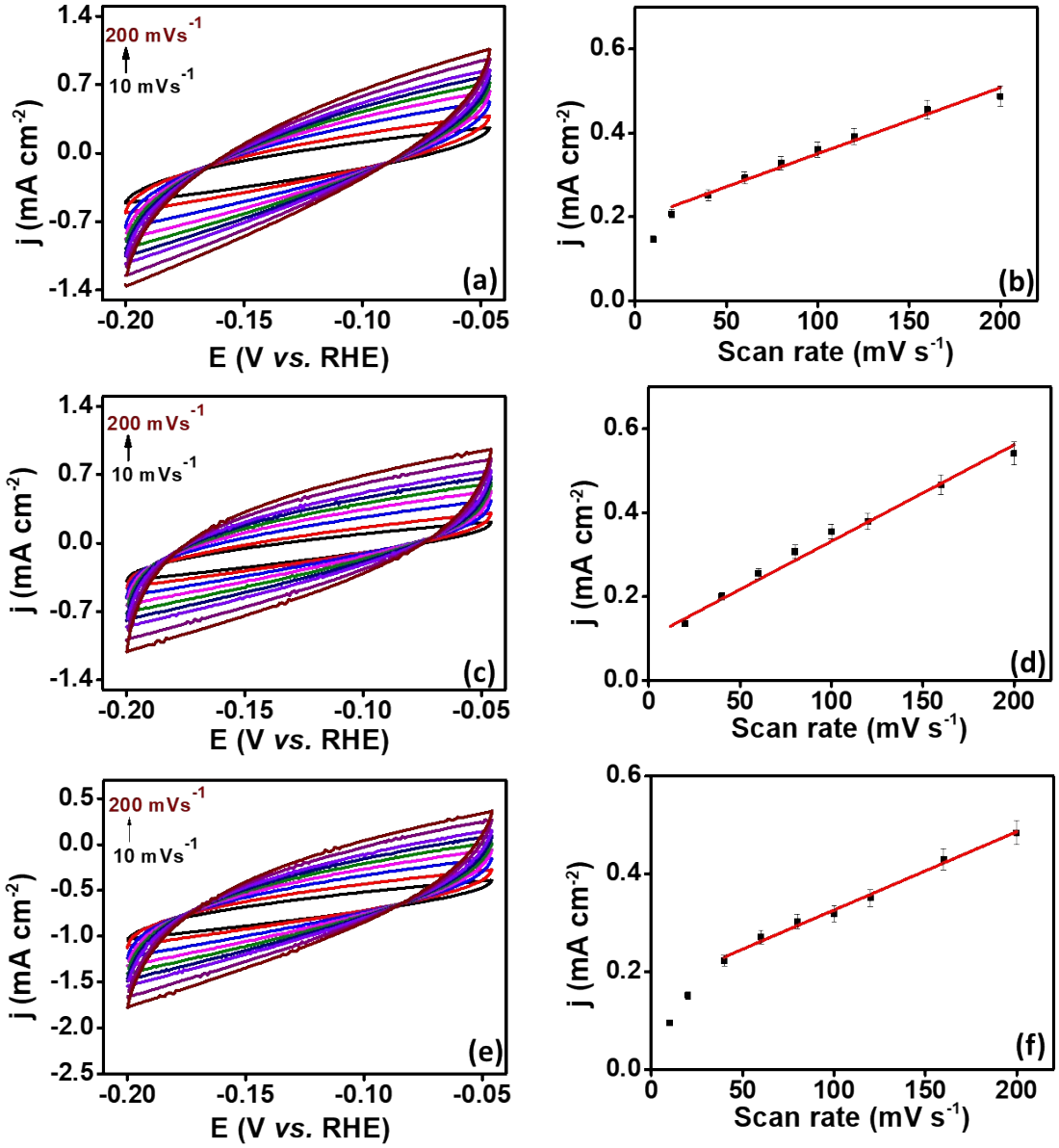

Fig. S14 (a, c,e) Cyclic voltammograms for $CoWO_4$ (8 h), $CoWO_4$ (12 h) and $CoWO_4$ (20 h) catalyst at different scan rates and (b, d,f) corresponding current density *vs.* scan rate plots extracted from the CVs respectively.

Table S4: Electrochemical surface area (ECSA) measurements.

S.No	Catalyst	Cdl (µF) at -0.121 V	ECSA (cm^{-2})	Roughness factor (a.u.)
1	$CoWO_4$ (8 h)	49.5	1.24	39.49
2	$CoWO_4$ (12 h)	72.2	1.80	57.32
3	$CoWO_4$ (20 h)	44.62	1.12	35.66

Table S5: Tafel slope values extracted from LSV of catalysts in N_2-saturated 0.1 M KOH		
S.No	**Catalyst**	**Tafel slope (mV dec^{-1})**
1	$CoWO_4$ (8 h)	274
2	$CoWO_4$ (12 h)	267
3	$CoWO_4$ (20 h)	271

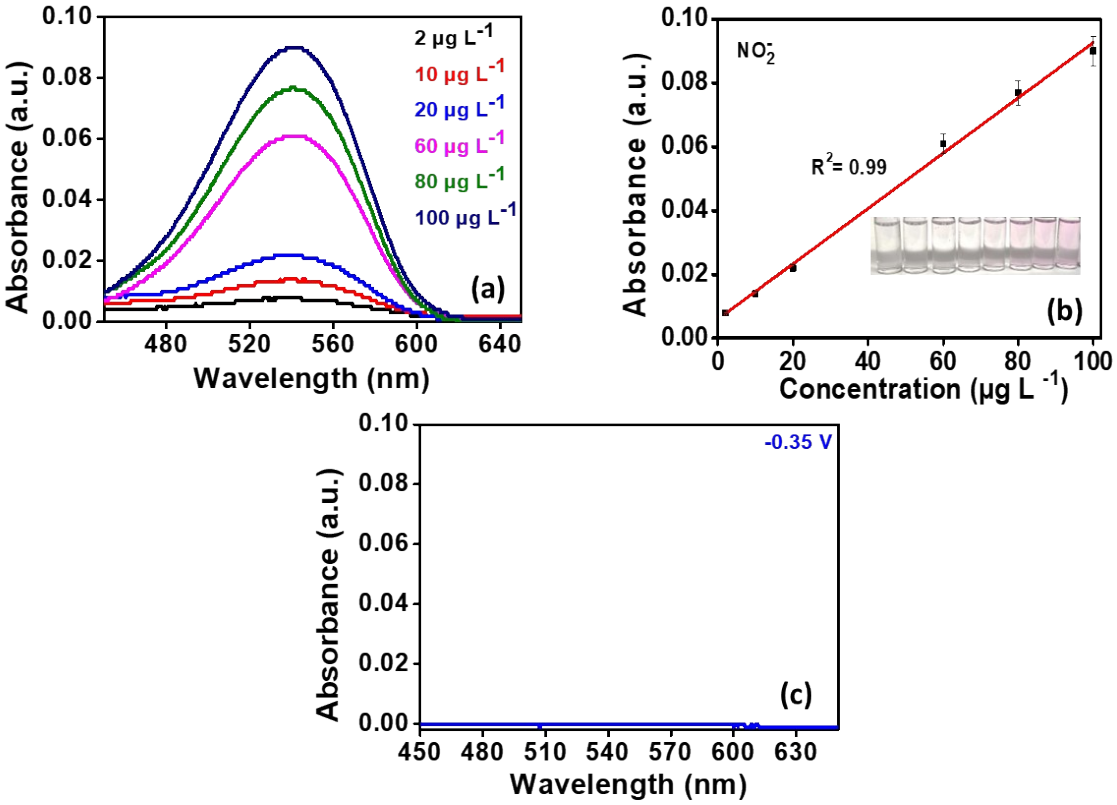

Fig. S15 (a) UV-Vis absorption spectra for various concentration of nitrite (b) Corresponding calibration curve for determining NO_2^- concentration at wavelength of 220 nm (c) UV-Vis absorption spectra of electrolyte after NRR electrolysis at -0.35 V *vs.* RHE.

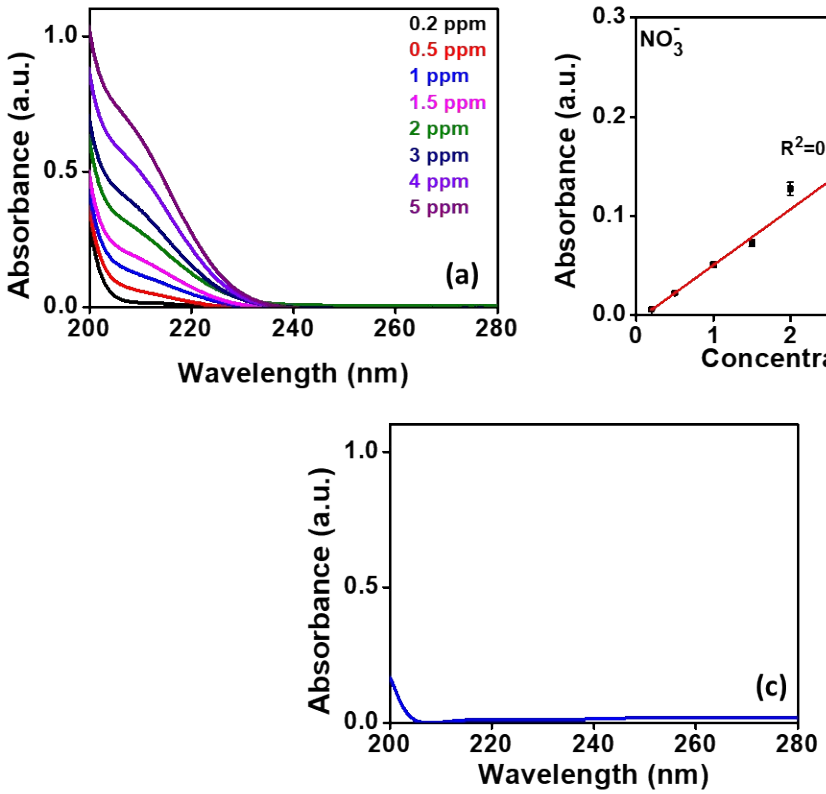

Fig. S16 (a) UV-Vis absorption spectra for various concentration of nitrate (b) Calibration curve for detection of NO_3^- at wavelength of 540 nm (c) UV-Vis spectra for determination of NO_3^- after electrolysis at a potential of -0.35 V using $CoWO_4$ (12 h) catalyst in 0.1 M KOH solution.

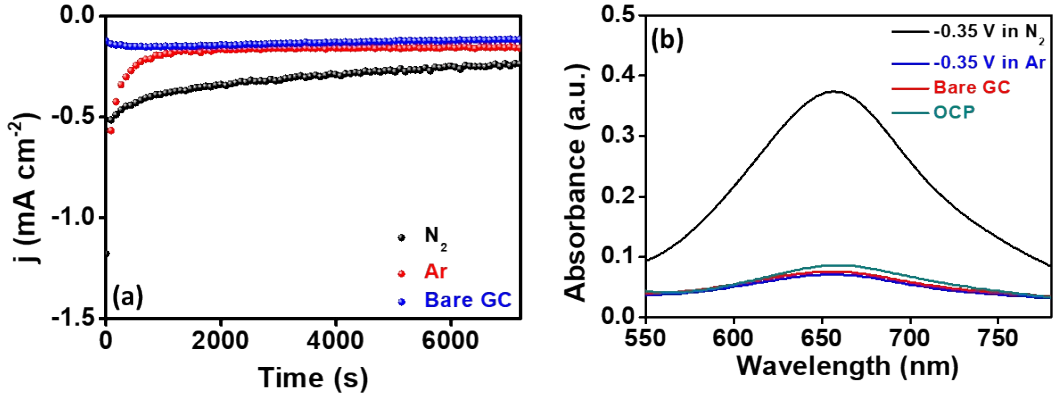

Fig. S17 (a) Chronoamperometric curves at potential of -0.35 V *vs*. RHE of $CoWO_4$ (12 h) catalyst in N_2 and Ar-saturated 0.1 M KOH solution and at bare glassy carbon electrode (GC) (b) its corresponding UV-Vis absorption spectra for NH_3.

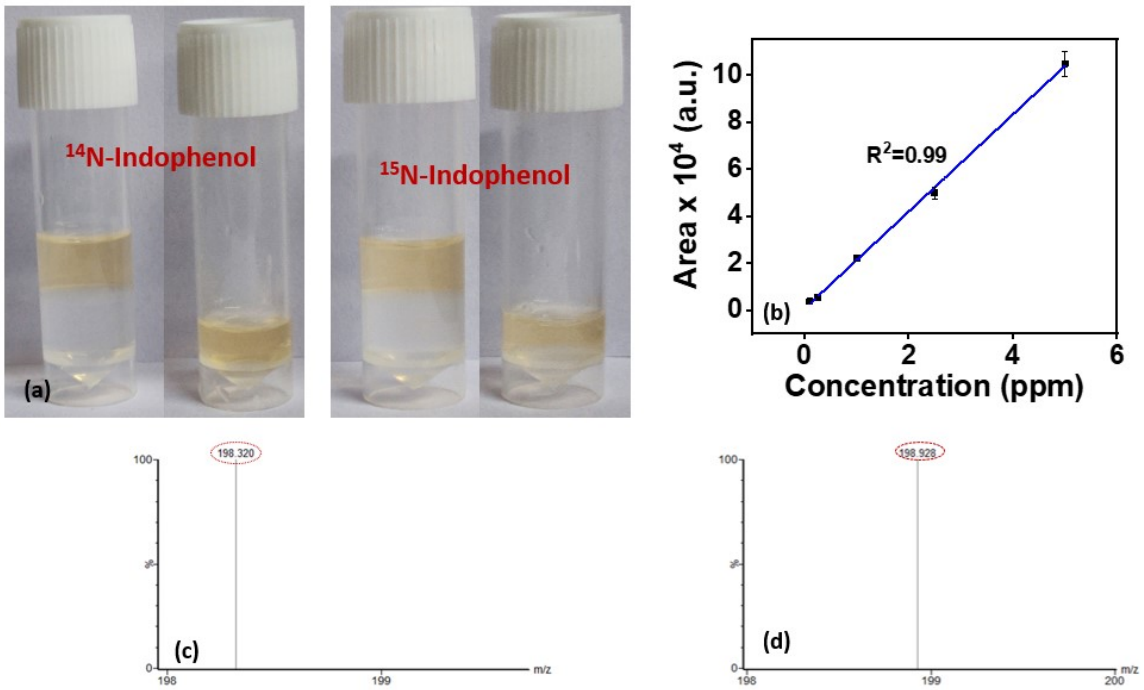

Fig. S18 (a) Photographs showing the extraction of Indophenol red from organic layer before LC-MS quantification for electrolyte samples, abundance of ^{14}N Indophenol and ^{15}N Indophenol for the electrolyte samples obtained after NRR and (c,d) its corresponding mass spectrum. (b) Calibration curves extracted from LC-MS of standard samples after Berthelot reaction.

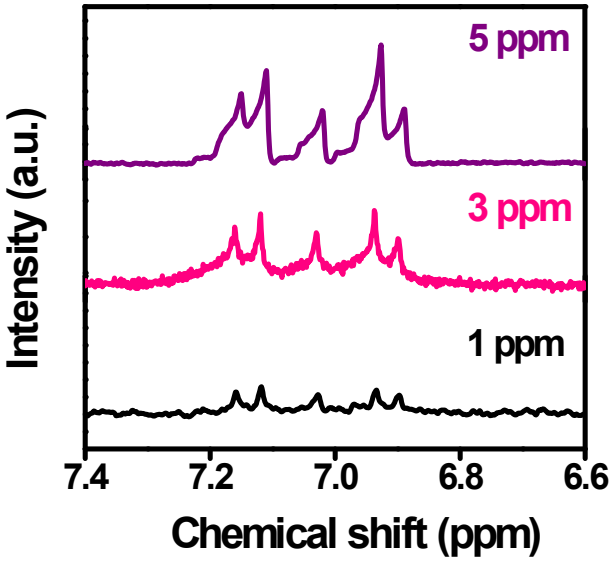

Fig. S19 ^{1}H-NMR spectra of standard equimolar mixture of $^{14}NH_4Cl$ and $^{15}NH_4Cl$ solutions with different concentrations ranging between 1 ppm to 5 ppm.

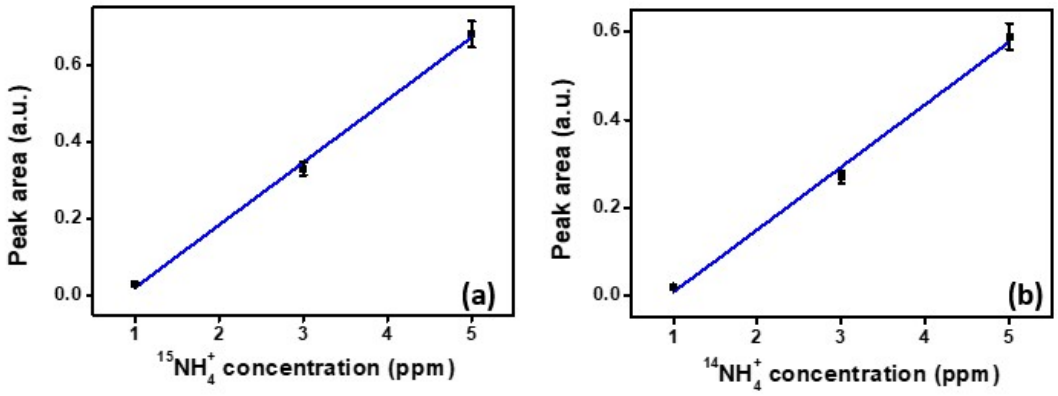

Fig. S20 Calibration curves for various standard concentration of NH_4^+ extracted from ^1H NMR spectra for (a) $^{15}NH_4^+$ and (b) $^{14}NH_4^+$ respectively.

Table S6: Comparison of NH_3 yield rates obtained after 2 h of e-NRR by $CoWO_4$ (12 h) at -0.35 V (*vs.* RHE) for isotope labelling experiment by different methods.			
S.No	**Method of detection**	**$^{14}NH_3$ concentration**	**$^{15}NH_3$ concentration**
1	Indophenol blue	663.49	667.86
2	^1H-NMR	664.55	655.08
3	LC-MS	662.65	660.96

Table S7: Comparison of NH_3 yield rate obtained after 2 h of NRR by $CoWO_4$ (12 h) at -0.35 V *vs.* RHE		
S.No	**Detection method**	**NH_3 yield rate ($\mu g\ h^{-1}\ mg_{cat}^{-1}$)**
1	Indophenol blue	667.86
2	Nessler's reagent	640.26

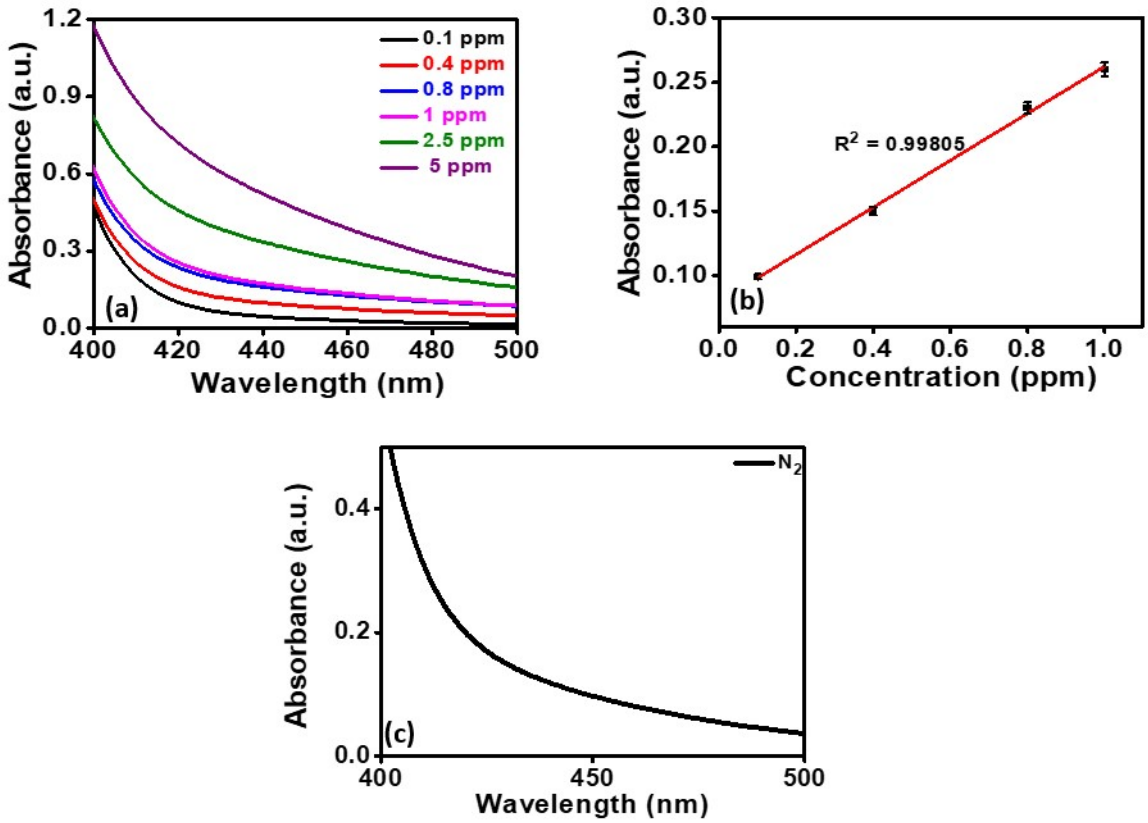

Fig. S21 (a) UV-Vis spectra for different concentration of Nessler's reagent and (b) its corresponding calibration curve for measurement. (c) UV-Vis spectra for Nessler's reagent obtained after electrolysis

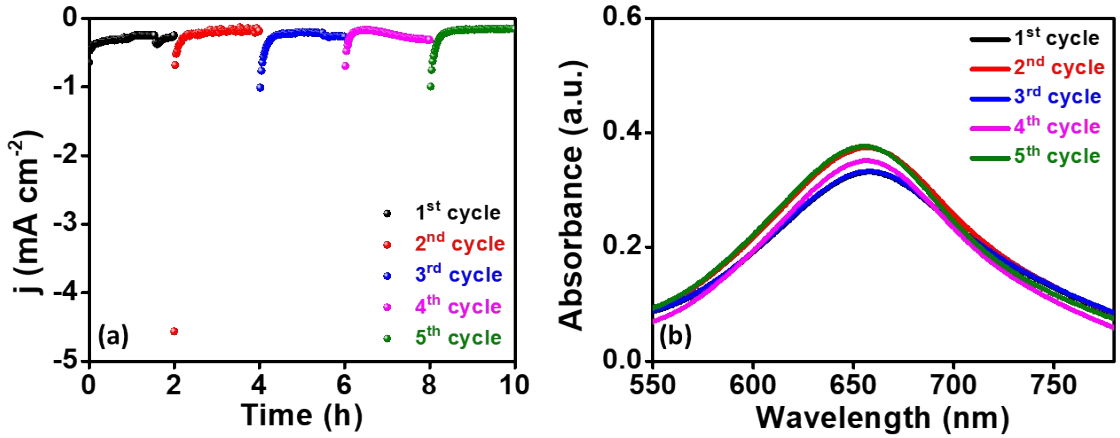

of 2 h for $CoWO_4$ (12 h).

Fig. S22 (a) Chronoamperometry curves for NRR stability tests for 5 consecutive cycles of 0.1 M KOH saturated solution of N_2 for $CoWO_4$ (12 h) catalyst at -0.35 V of applied potential, (b) and its corresponding UV-Vis. absorbance curves.

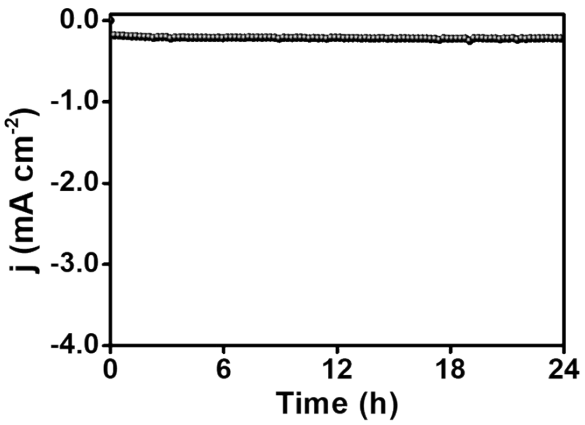

Fig. S23 Chronoamperometry curve for $CoWO_4$ (12 h) acquired for 24 h continuous NRR in N_2-saturated 0.1 M KOH.

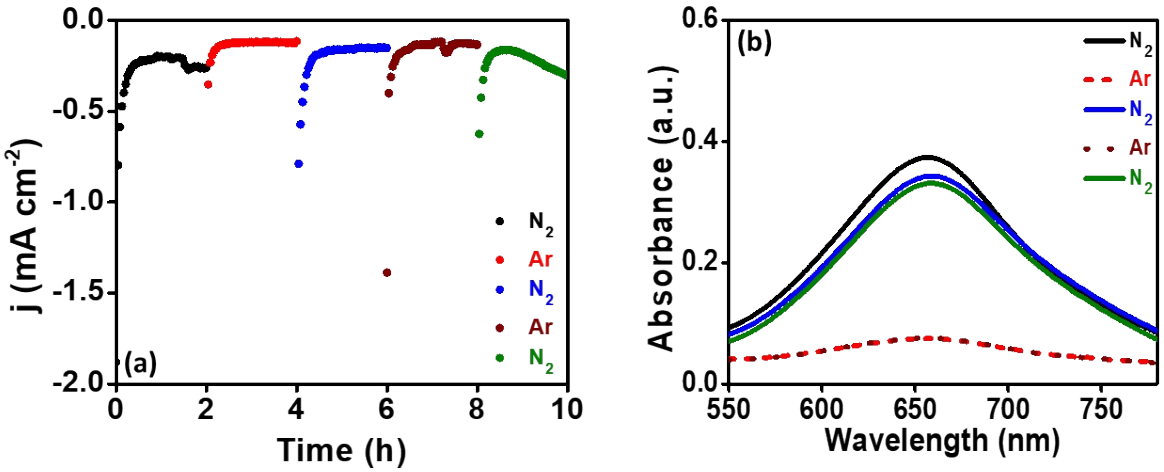

Fig. S24 (a) Chronoamperometry curves for NRR stability tests for 5 alternate cycles of 0.1 M KOH saturated solution of N_2 and Ar for $CoWO_4$ (12 h) catalyst at -0.35 V of applied potential. (b) and its corresponding UV-Vis. absorbance curves.

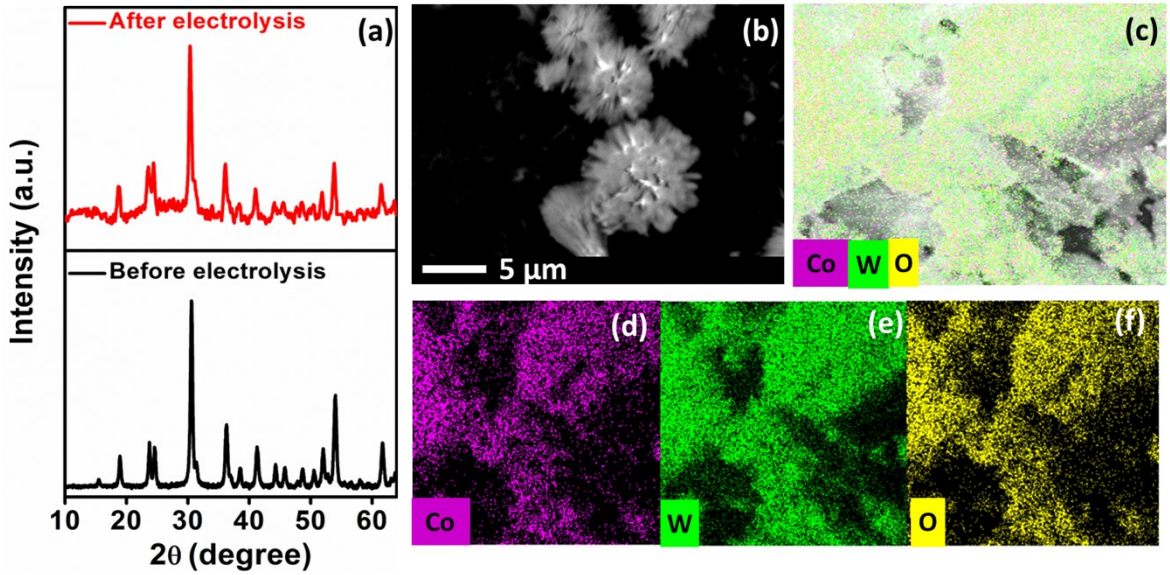

Fig. S25 (a) XRD analysis before and after stability test (b) Post SEM image and EDS dot mapping image for $CoWO_4$ (12 h) catalyst after NRR stability test showing presence of (c) all the elements in scanned area, (d) Co, (e) W and (f) O elements respectively.

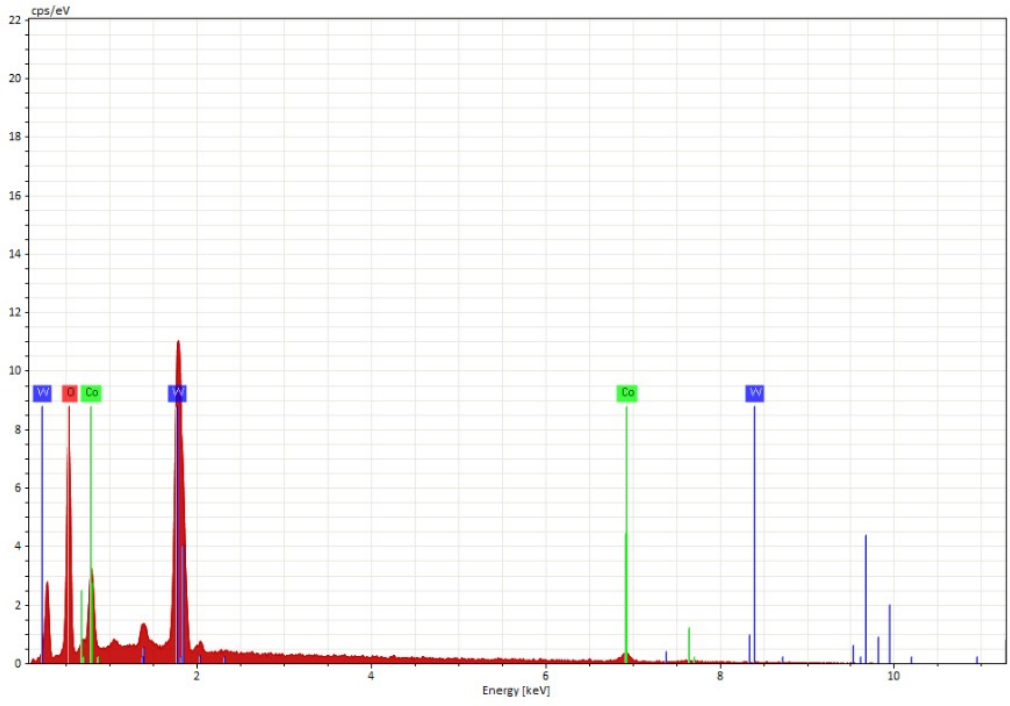

Fig. S26 EDS spectra of $CoWO_4$ (12 h) showing presence of Co, W and O after NRR stability experiment.

Table S8: Post EDS composition analysis (%) before and after NRR stability test for $CoWO_4$ (12 h)				
	Before electrolysis		**After electrolysis**	
Elements	Weight %	Atomic %	Weight %	Atomic %
Cobalt	10.648	8.822	11.823	9.21
Tungsten	65.145	17.301	61.9	15.448
Oxygen	24.208	73.877	26.275	75.35

Table S9: Comparison of activity of recent reported catalysts towards NRR

Catalyst	Electrolyte	R_{NH3} (μg h^{-1} mg^{-1}_{cat})	E *vs.* RHE	F.E. (%)	Ref.
FeTPPCl	0.1 M Na_2SO_4	18.28 ± 1.6 µ	-0.3 V	16.76 ± 0.9	[8]
FeS2@GO	0.1 M Na_2SO_4	27.9 @ -0.7 V	-	6.8@ -0.6 V	[9]
2D In-MOF	0.1 M Na_2SO_4	64.73	-	12.23	[10]
VN@NSC-900	0.1 M HCl	20.5	-0.3 V	8.6	[11]
FL-VS2	0.1 M HCl	34.62	-0.7 V	2.09 @ -0.6 V	[12]
CoPi/NPCS	0.1 M KOH	20.5	-0.2 V	7.07	[13]
CoPi/HSNPC	0.1M KOH	16.48	-0.2 V	4.46	[14]
Co/C-900	0.1 M KOH	4.66 µmol h^{-1} cm^{-2}	0.3 V	11.53	[15]
$NiWO_4$	0.1M HCl	48.86	-0.3	19.32	[16]
	0.1 M Na_2SO_4	28.4	-0.3	10.18	
W-NO/NC	0.5 M $LiClO_4$	123.5	-0.7	8.35	[17]
Co-SAs/NC	0.005 M H_2SO_4	16.9	-0.25	7.5 @-0.45 V	[18]
Sulfur vacancy-rich MoS_2	0.1 M Na_2SO_4	60.27	-0.6 V	12.22	[19]
$NiPS_3$	0.1 M Na_2SO_4	118	-0.4 V	17	[20]
$NiO@TiO_2$	0.05 M Na_2SO_4	10.75	-0.4 V	9.83	[21]
AuPd NSs	0.1 M Na_2SO_4	16.9	−0.3 V	15.9	[22]
Pd/PdO (O-M)	0.1 M KOH	11.0	0.0 V	22.2	[23]
Bi–MoO_x@RGO	0.10 M Na_2SO_4	19.93	−0.3 V	17.17	[24]
S/N-C-11	0.1 M KOH	6.9396 µmol cm^{-2} h^{-1}	− 0.4 V	22.74	[25]
OVs-Bi_2MoO_6	0.1 M HCl	24.38	−0.3 V	14.1	[26]
Cu_2SnS_3	0.1 M Na_2SO_4	8.22	−0.4 V	8.87	[27]
$Ti_3C_2T_x$ MXene	0.1 M HCl	88.3±1.7	−0.35 V	9.3±0.4	[28]
$CoWO_4$ (12 h)	**0.1 M KOH**	**667.86**	**-0.35**	**22.34**	**This work**

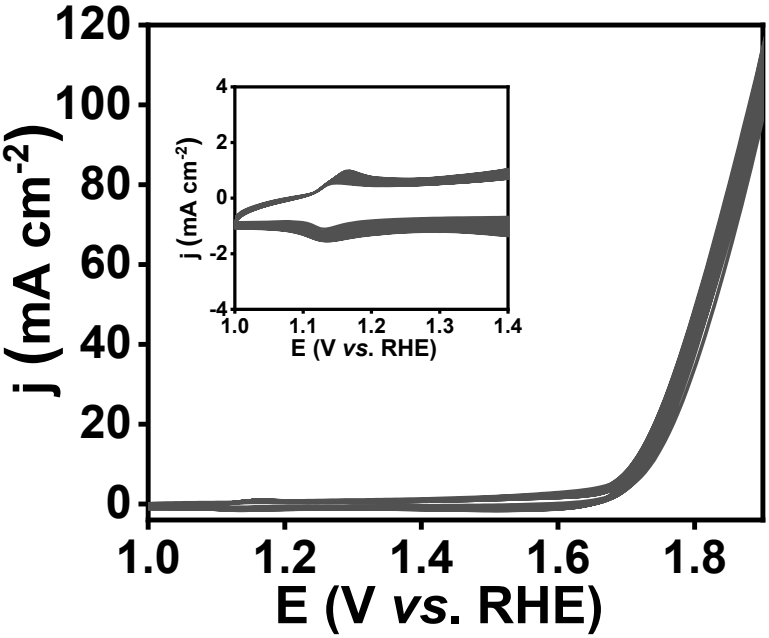

Fig. S27 Cyclic voltammetry at scan rate of 50 mV s^{-1} for 50 cycles (inset showing redox peaks for Co^{2+} / Co^{3+}).

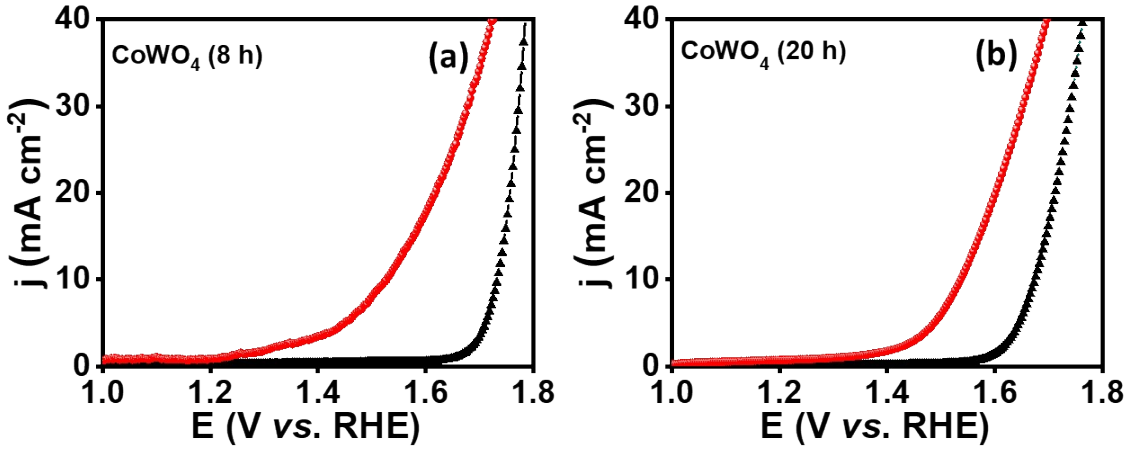

Fig. S28 Comparison of GOR and OER activity of $CoWO_4$ (8 h) and $CoWO_4$ (12 h).

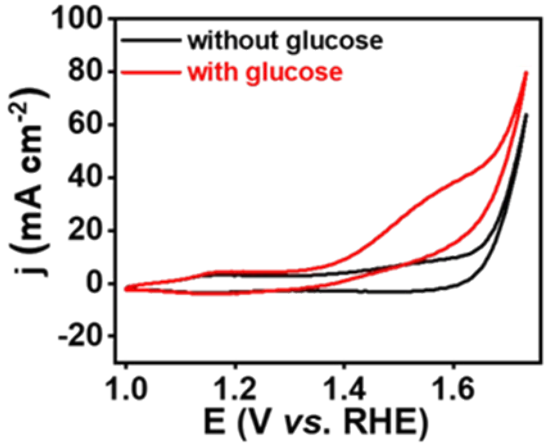

Fig. S29 CV curves for $CoWO_4$ (12 h) catalyst with and without glucose at a scan rate of 100 mVs^{-1}.

Table S10: HRMS analysis

S.No.	Compounds	Molecular mass	adducts
1	Glucose	180	
2	Gluconolactone	178	179 (M+H)
3	Gluconic acid	196	196 (M+H) 225 (M+K+H_2O-CO) 226 (M+K+H_2O+H-CO)
4	Glucaric acid	210	236 (M+K+H_2O+3H-CO) 280 (M+2K+H_2O+2H-CO) 296 (M+2K+2H_2O-CO)
5	Guluronic acid	194	213(M+K-H_2O) 215(M+K+2H-H_2O)

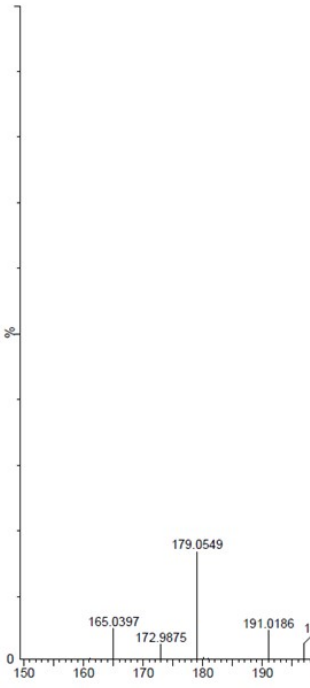

Fig. S30 HRMS data of glucose oxidation.

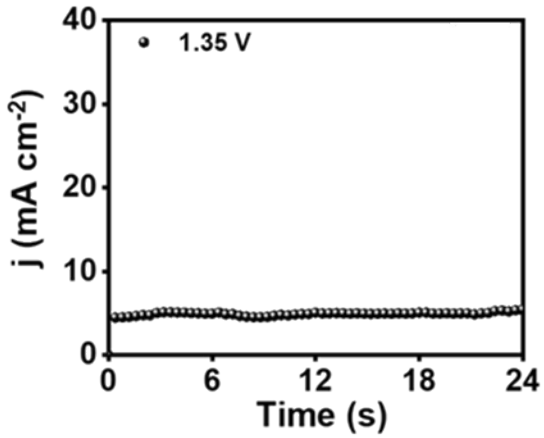

Fig. S31 Chronoamperometric curves for glucose oxidation obtained at -1.35 V *vs*. RHE for 24 h.

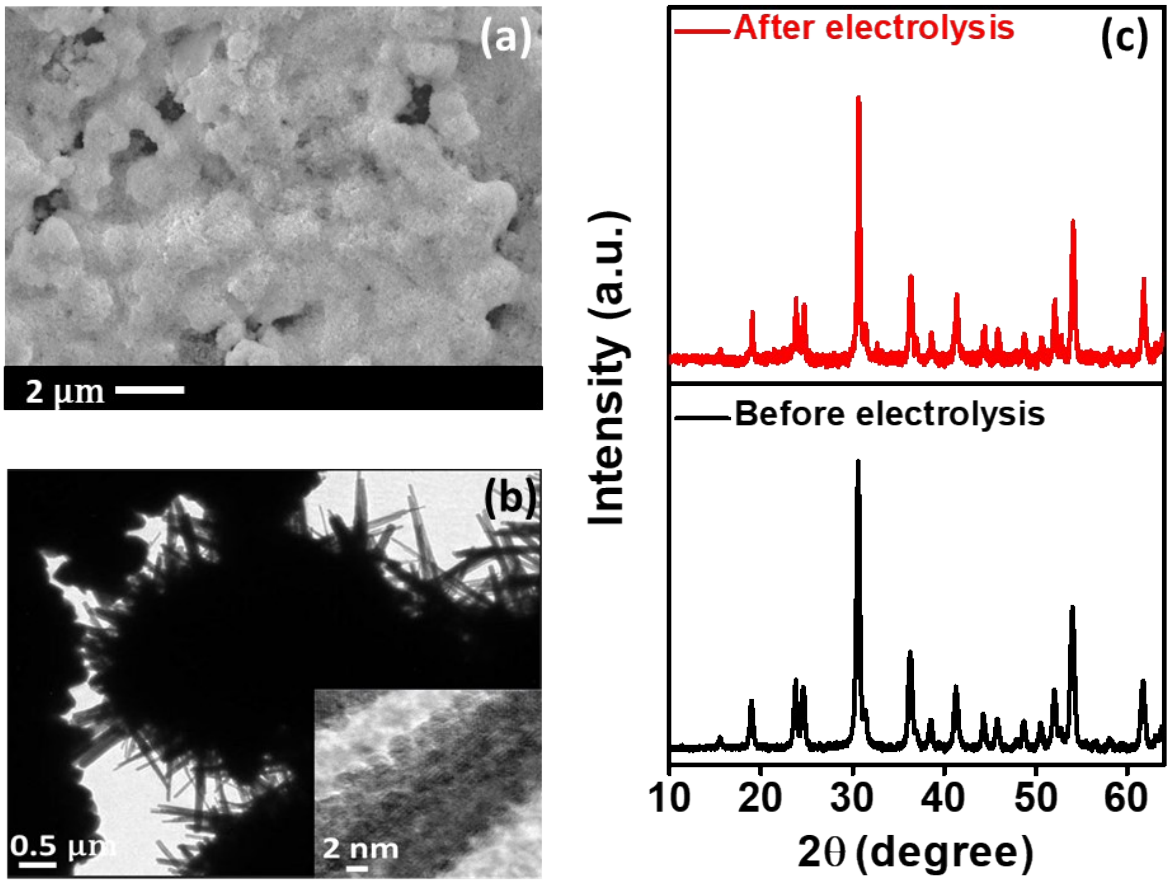

Fig. S32 (a) SEM and (b) TEM image of $CoWO_4$ (inset: HR-TEM) after stability test for glucose oxidation, (c) XRD pattern for CoWO4 (12 h) before and after glucose electrolysis.

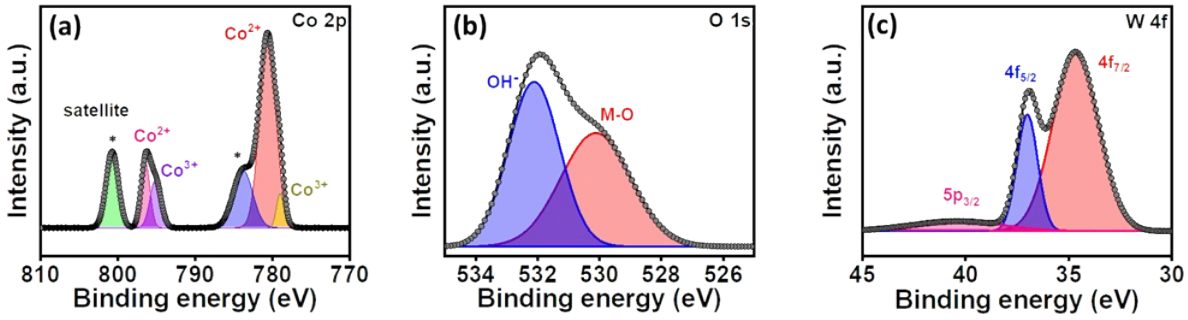

Fig. S33 XP spectra of (a) Co 2p, (b) O 1s and (c) W 4f of $CoWO_4$ (12 h) catalyst respectively after glucose oxidation.

Table S11. Comparison of $CoWO_4$ (12 h) catalyst with others previously reported catalyst for electrochemical glucose oxidation.

Catalyst	Voltage	Current	Product	Ref.

	(V)	density (mA cm^{-2})		
Fe_2P/SSM	1.22 1.51 1.58	10 50 100	-	[29]
NiFeOx-NF	1.33 1.39	50 100	Gluconic acid, Glucaric acid,	[30]
$Cu(OH)_2$	0.74 0.83 0.92	10 50 100	Gluconic acid	[31]
CF@CoNC-2T	0.90	100	Gluconic acid, guluronic acid, glucaric acid	[32]
Ni–MoS_2 NPs	1.67	10	-	[33]
NiV(2:1)P/Pi-VC	1.3	10	Gluconolactone, Gluconic acid, Glucaric acid	[34]
$Fe_{0.1}$-$CoSe_2$/CC	0.72	10	Gluconate	[35]
CNT@Co/CoP	1.42	10	Gluconate, gluconic acid	[36]
Co@NPC	1.56	10	Lactic acid, Formic acid	[37]
$CoWO_4$(12 h)	**1.44**	**10**	**Gluconolactone, Gluconic acid, Glucaric acid, Guluronic acid**	**This work**

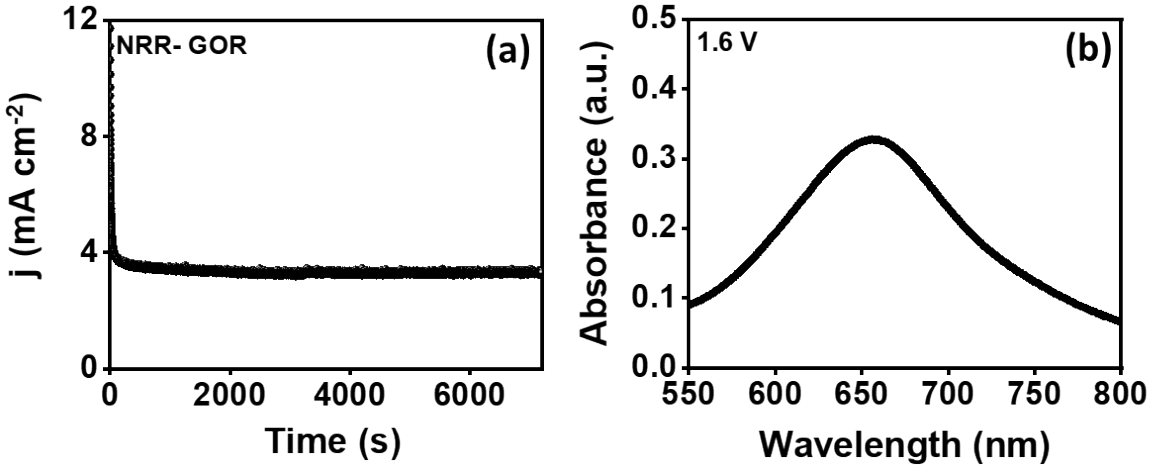

Fig. S34 (a) Chronoamperometry recorded at 1.6 V and (b) corresponding UV-Vis spectra recorded for NRR-GOR full cell

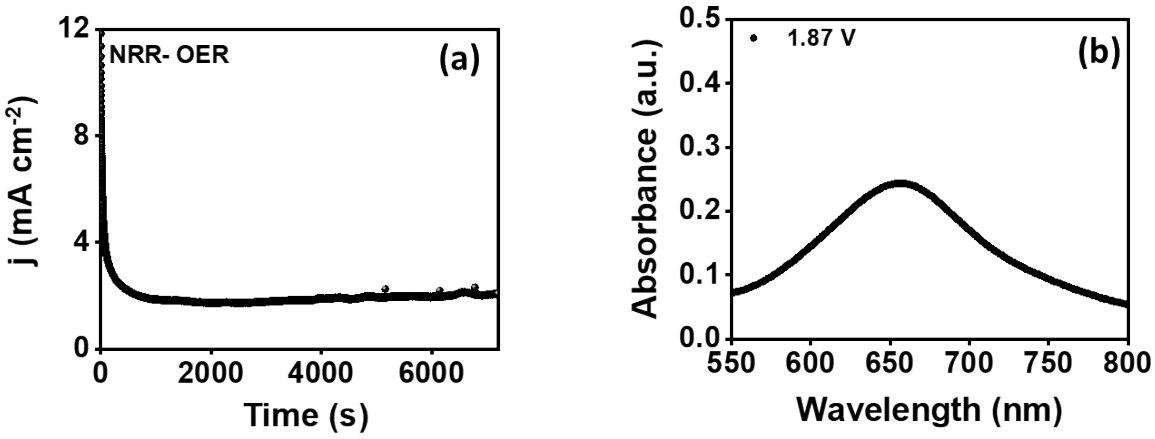

Fig. S35 (a) Chronoamperometry recorded at 1.87 V and (b) corresponding UV-Vis spectra recorded for NRR-OER full cell

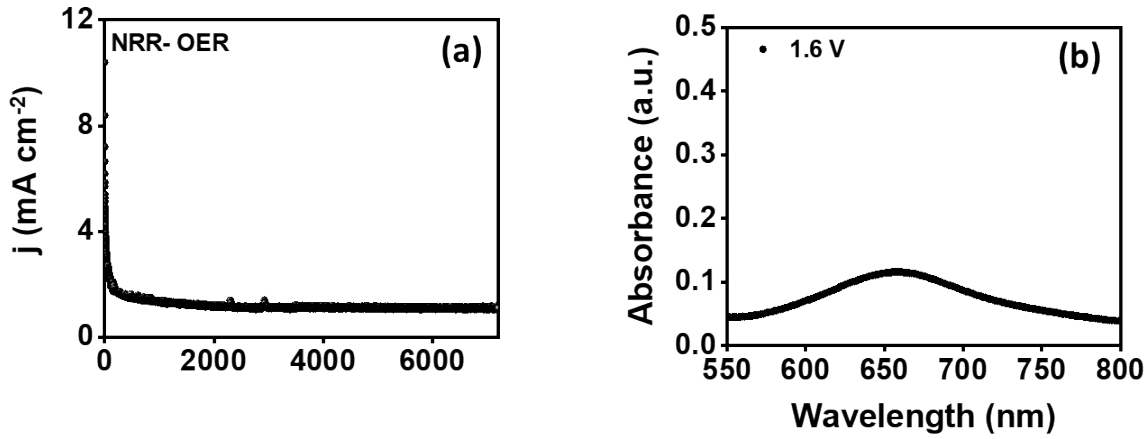

Fig. S36 (a) Chronoamperometry recorded at 1.6 V and (b) corresponding UV-Vis spectra recorded for NRR-OER full cell

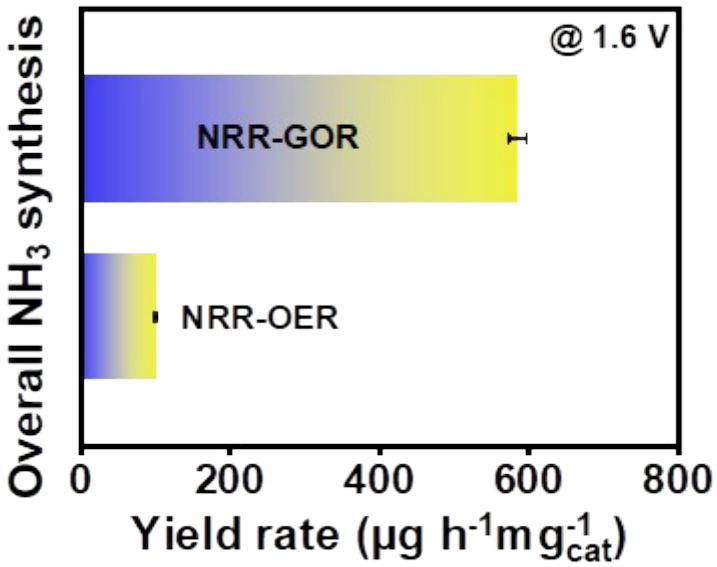

Fig. S37 NH_3 yield for NRR-GOR and NRR-OER after electrolysis at 1.6 V.

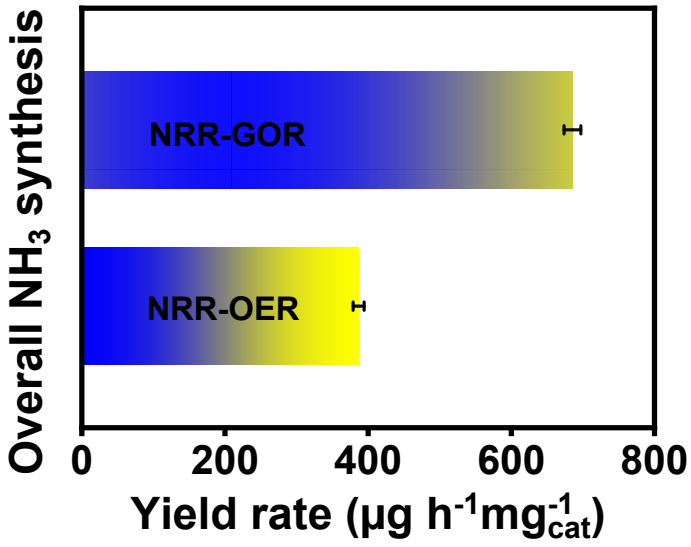

Fig. S38 NH_3 yield for NRR-GOR and NRR-OER full cell conditions after electrolysis at 1.87 V.

References

1. Y. Zhao, R. Shi, X. Bian, C. Zhou, Y. Zhao, S. Zhang, F. Wu, G. I. N. Waterhouse, L.-Z. Wu, C.-H. Tung and T. Zhang, *Adv. Sci.*, 2019, **6**, 1802109.
2. S. Z. Andersen, V. Čolić, S. Yang, J. A. Schwalbe, A. C. Nielander, J. M. McEnaney, K. Enemark-Rasmussen, J. G. Baker, A. R. Singh, B. A. Rohr, M. J. Statt, S. J. Blair, S. Mezzavilla, J. Kibsgaard, P. C. K. Vesborg, M. Cargnello, S. F. Bent, T. F. Jaramillo, I. E. L. Stephens, J. K. Nørskov and I. Chorkendorff, *Nature*, 2019, **570**, 504-508.
3. S. E. Saji, H. Lu, Z. Lu, A. Carroll and Z. Yin, *Small Methods*, 2021, **5**, 2000694.
4. G. W. Watt and J. D. J. A. C. Chrisp, *J. Anal. Chem.*, 1952, **24**, 2006-2008.
5. L. Li, C. Tang, D. Yao, Y. Zheng and S.-Z. Qiao, *ACS Energy Lett.*, 2019, **4**, 2111-2116.
6. D. Ekeberg, G. Ogner, M. Fongen, E. J. Joner and T. Wickstrøm, *J. Environ. Monit.*, 2004, **6**, 621-623.
7. J. Choi, B. H. R. Suryanto, D. Wang, H.-L. Du, R. Y. Hodgetts, F. M. Ferrero Vallana, D. R. MacFarlane and A. N. Simonov, *Nat. Commun.*, 2020, **11**, 5546.
8. X. Yang, S. Sun, L. Meng, K. Li, S. Mukherjee, X. Chen, J. Lv, S. Liang, H.-Y. Zang, L.-K. Yan and G. Wu, *Appl. Catal. B*, 2021, **285**, 119794.
9. L. Gao, C. Guo, M. Zhao, H. Yang, X. Ma, C. Liu, X. Liu, X. Sun and Q. Wei, *ACS Appl. Mater. Interfaces*, 2021, **13**, 50027-50036.
10. Y. Sun, B. Xia, S. Ding, L. Yu, S. Chen and J. Duan, *J. Mater. Chem. A*, 2021, **9**, 20040-20047.
11. X. W. Lv, Y. Liu, Y. S. Wang, X. L. Liu and Z. Y. Yuan, *Appl. Catal. B*, 2021, **280**.
12. L. Zhao, R. Zhao, Y. Zhou, X. Wang, X. Chi, Y. Xiong, C. Li, Y. Zhao, H. Wang, Z. Yang and Y.-M. Yan, *J. Mater. Chem. A*, 2021, **9**, 24985-24992.
13. J. T. Ren, L. Chen, H. Y. Wang and Z. Y. Yuan, *ACS Appl Mater Interfaces*, 2021, **13**, 12106-12117.
14. J.-T. Ren, L. Chen, Y. Liu and Z.-Y. Yuan, *J. Mater. Chem. A*, 2021, **9**, 11370-11380.
15. A. Liu, X. Liang, Q. Yang, X. Ren, M. Gao, Y. Yang and T. Ma, *ChemElectroChem*, 2020, **7**, 4900-4905.
16. J. Wang, H. Jang, G. Li, M. G. Kim, Z. Wu, X. Liu and J. Cho, *Nanoscale*, 2020, **12**, 1478-1483.

17. Y. Gu, B. Xi, W. Tian, H. Zhang, Q. Fu and S. Xiong, *Adv. Mater.*, 2021, **33**, e2100429.
18. S. Zhang, Q. Jiang, T. Shi, Q. Sun, Y. Ye, Y. Lin, L. R. Zheng, G. Wang, C. Liang, H. Zhang and H. Zhao, *ACS Appl. Energy Mater.*, 2020, **3**, 6079-6086.
19. H. Fei, T. Guo, Y. Xin, L. Wang, R. Liu, D. Wang, F. Liu and Z. Wu, *Appl. Catal. B*, 2022, **300**, 120733.
20. B. Vedhanarayanan, C.-c. Chiu, J. Regner, Z. Sofer, K. C. Seetha Lakshmi, J.-Y. Lin and T.-W. Lin, *Chem. Eng. J.*, 2022, **430**, 132649.
21. Y. Tian, B. Chang, G. Wang, L. Li, L. Gong, B. Wang, R. Yuan and W. Zhou, *J. Mater. Chem. A*, 2022, **10**, 2800-2806.
22. S. Yin, S. Liu, H. Zhang, S. Jiao, Y. Xu, Z. Wang, X. Li, L. Wang and H. Wang, *ACS Appl. Mater. Interfaces*, 2021, **13**, 20233-20239.
23. Q. Chen, X. Zhou, X. Zhang, W. Luo, S. Yang, Y. Ge, D. Cai, H. Nie and Z. Yang, *ACS Appl. Mater. Interfaces*, 2022, **14**, 20988-20996.
24. Y. Wan, Z. Wang, M. Zheng, J. Li and R. Lv, *J. Mater. Chem. A*, 2023, **11**, 818-827.
25. B. Wei, Y. Liang, L. Li and C. Yao, *J. Electron. Mater.*, 2023, **52**, 2227-2235.
26. Y. Zhang, Y. Wang, X. Mou, C. Song and D. Wang, *Electrochim. Acta*, 2023, **439**, 141661.
27. X. He, Z. Ling, X. Peng, X. Yang, L. Ma and S. Lu, *Electrochem. Commun.*, 2023, **148**, 107441.
28. X. Peng, R. Zhang, Y. Mi, H.-T. Wang, Y.-C. Huang, L. Han, A. R. Head, C.-W. Pao, X. Liu, C.-L. Dong, Q. Liu, S. Zhang, W.-F. Pong, J. Luo and H. L. Xin, **n/a**, e202201385.
29. P. Du, J. Zhang, Y. Liu and M. Huang, *Electrochem. Commun.*, 2017, **83**, 11-15.
30. W.-J. Liu, Z. Xu, D. Zhao, X.-Q. Pan, H.-C. Li, X. Hu, Z.-Y. Fan, W.-K. Wang, G.-H. Zhao, S. Jin, G. W. Huber and H.-Q. Yu, *Nat. Commun.*, 2020, **11**, 265.
31. Y. Zhang, B. Zhou, Z. Wei, W. Zhou, D. Wang, J. Tian, T. Wang, S. Zhao, J. Liu, L. Tao and S. Wang, *Adv. Mater.*, 2021, **33**, 2104791.
32. Y. Xin, F. Wang, L. Chen, Y. Li and K. Shen, *Green Chemistry*, 2022, **24**, 6544-6555.
33. X. Liu, P. Cai, G. Wang and Z. Wen, *Int. J. Hydrogen Energy*, 2020, **45**, 32940-32948.
34. N. Thakur, D. Mehta, A. Chaturvedi, D. Mandal and T. C. Nagaiah, *J. Mater. Chem. A*, 2023, DOI: 10.1039/D3TA02133E.
35. D. Zheng, J. Li, S. Ci, P. Cai, Y. Ding, M. Zhang and Z. Wen, *Appl. Catal. B*, 2020, **277**, 119178.
36. Y. Zhang, Y. Qiu, Z. Ma, Y. Wang, Y. Zhang, Y. Ying, Y. Jiang, Y. Zhu and S. Liu, *J. Mater. Chem. A*, 2021, **9**, 10893-10908.
37. D. Li, Y. Huang, Z. Li, L. Zhong, C. Liu and X. Peng, *Chem. Eng. J.*, 2022, **430**, 132783.